Molecular Basis for the Stereoselective Ammoniolysis of *N*-Alkyl Aziridine-2-Carboxylates Catalyzed by *Candida antarctica* Lipase B

Jae-Hoon Park,[a] Hyun-Joon Ha,*[a] Won Koo Lee,*[b] Tobie Généreux-Vincent,[c] and Romas J. Kazlauskas*[c, d]

Dedicated to Kalle Hult on the occasion of his 65th birthday

Candida antarctica lipase B catalyzed the stereoselective ammoniolysis of *N*-alkyl aziridine-2-carboxylates in *t*BuOH saturated with ammonia and yielded the (2*S*)-aziridine-2-carboxamide and unreacted (2*R*)-aziridine-2-carboxylate. Varying the N-1 substituent on the aziridine ring changed the rate and stereoselectivity of the reaction. Substrates with a benzyl substituent or a (1′*R*)-1-phenylethyl substituent reacted approximately ten times faster than substrates with a (1′*S*)-1-phenylethyl substituent. Substrates with a benzyl substituent showed little stereoselectivity (*E* = 5–7) while substrates with either a (1′*R*)- or (1′*S*)-1-phenylethyl substituent showed high stereoselectivity (*D* > 50). Molecular modeling by using the current paradigm for enantioselectivity—binding of the slow enantiomer by an ex-change-of-substituents orientation—could not account for the experimental results. However, modeling an umbrella-like-inversion orientation for the slow enantiomer could account for the experimental results. Steric hindrance between the methyl in the (1′*S*)-1-phenylethyl substituent and Thr138 and Ile189 in the acyl-binding site likely accounts for the slow reaction. Enantioselectivity likely stems from an unfavorable interaction of the methine hydrogen with Thr40 for the slow enantiomer and from subtle differences in the orientations of the other three substituents. This success in rationalizing the enantio-selectivity supports the notion that an umbrella-like-inversion orientation can contribute to enantioselectivity in lipases.

Introduction

Enantiopure aziridine-2-carboxylates are useful precursors for the synthesis of amine-containing molecules, such as natural and unnatural amino acids, amino alcohols and α,β-diamines.[1] Current routes to enantiopure aziridine-2-carboxylates include synthesis from enantiopure precursors and resolution through diastereomers by using chromatography, ester cleavage or crystallization.[2] Enzyme-catalyzed kinetic resolutions are an attractive alternative, but initial attempts with pig pancreatic lipase (PPL) or *Candida rugosa* lipase (CRL) gave either low yields or low enantiomeric purities. Separation of the product aziridine carboxylic acid from the starting ester required an inconvenient chromatography.[3]

In this paper, we report an efficient and highly stereoselective ammoniolysis of *N*-alkyl aziridine-2-carboxylates using the enzyme *Candida antarctica* lipase B (CAL-B). Although the *N*-alkyl group is far (three bonds) from the reaction center, the nature of this group was critical to achieving high enantioselectivity. In addition, by using an ammoniolysis[4] instead of a hydrolysis for the resolution allows separation of the water-soluble product, aziridine carboxamide, from the hexane-soluble starting aziridine carboxylate ester by partitioning between water and hexane.

To rationalize the enantiopreference of CAL-B toward *N*-alkyl aziridine-2-carboxylates and the influence of the *N*-alkyl substituent on reaction rate and enantioselectivity, we used molecular modeling. The current paradigm of how the fast- and slow-reacting enantiomers orient in the active site is that the stereocenters are in identical positions, but two substituents exchange locations (Figure 1). Unfortunately, this paradigm suggested sterically impossible orientations for the slow enantiomer and could not account for the experimental results obtained in this study.

Although the paradigm of exchanged substituents is widely accepted,[5–7] X-ray crystal structures of enantiomers bound to active sites show another possibility—an umbrella-like-inver-

[a] J.-H. Park, Prof. H.-J. Ha
Department of Chemistry and Protein Research Center for Bio-Industry
Hankuk University of Foreign Studies, Yongin, Kyunggi-Do, 449-791 (Korea)
Fax: (+ 82) 31-3331696
E-mail: hjha@hufs.ac.kr

[b] Prof. W. K. Lee
Department of Chemistry, Sogang University
Seoul, 121-742 (Korea)
Fax: (+ 82) 2-701096
E-mail: wonkoo@sogang.ac.kr

[c] T. Généreux-Vincent, Prof. R. J. Kazlauskas
Department of Chemistry, McGill University
Montréal, Québec, H3A 2K6 (Canada)

[d] Prof. R. J. Kazlauskas
Department of Biochemistry, Molecular Biology and Biophysics
The Biotechnology Institute, 1479 Gortner Avenue
Saint Paul, MN, 55108 (USA)
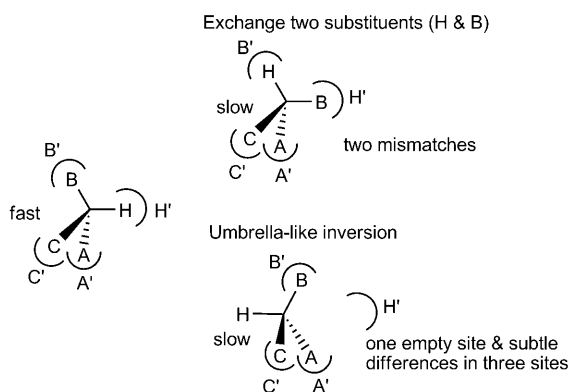Fax: (+ 1) 612-625-5780
E-mail: rjk@umn.edu

Figure 1. Two ways that the slow enantiomer that can fit in a site matches the fast-reacting enantiomer. For the fast enantiomer (left structure) all four interactions between the substituents (H, A, B, C) and the binding sites (H′, A′, B′, C′) match. To fit the slow enantiomer while preserving the location of the stereocenter (top right structure) requires exchanging two substituents, H and B in this example; there are five other possibilities. Only two substituents can match their binding sites. Another way to fit the slow enantiomer is through an umbrella-like inversion (bottom right structure) that leaves one site empty. This second possibility creates only one mismatch, but displaces the stereocenter.

sion orientation (Figure 1). Our previous survey[8] showed that in most cases (sixteen out of eighteen structures) enantiomers did not bind to active sites in an exchange-of-substituents orientation, but in an umbrella-like-inversion orientation. In this orientation, three of the four substituents at the stereocenter lie in similar positions. The fourth substituent, usually hydrogen, points in opposite directions. This orientation is likely energetically more favorable—it retains the interactions for three of the substituents instead of only for two.

In the previous paper,[8] we called this orientation a mirror-image-binding orientation, but we now prefer the more descriptive umbrella-like inversion. Since enantiomers are mirror images of each other, all examples of enantiomers bound to the same active site could be called mirror-image-binding orientations. The difference is that for exchange of substituents the mirror plane cuts through the stereocenter, while for the umbrella-like binding the mirror plane is next to the stereocenter. The phrase umbrella-like orientation avoids this potential confusion. Bentley[5] used an alternative phrase—enantiomer superposition—but this term can also be confused with exchange of substituents because it also involves superposition of enantiomers.

Although this umbrella-like orientation is common, it can be ignored in many cases because it is not catalytically productive. For example, alcohol oxidations involve removal of hydride from the stereocenter. The opposite orientation of the hydrogen in the two umbrella-like orientations makes oxidation impossible in one of these orientations. Only orientations that lead to products can lower the enantioselectivity of a reaction. In a more general case, any reaction that creates or destroys a stereocenter will involve bond making or bond breaking at the stereocenter. These reactions presumably require precise position-

ing of the stereocenter, so the displacement of the stereocenter in the umbrella-like orientation renders it unreactive. For these reactions, the current paradigm of enantioselectivity—exchange-of-substituents—works well.

However, this umbrella-like orientation might be important for lipase-catalyzed reactions. These enantioselective reactions do not occur at the stereocenter, but near a stereocenter, and do not create or destroy a stereocenter. They only preserve an existing stereocenter. The reacting group lies within one of the substituents shown in Figure 1. Thus, lipase-catalyzed reactions might tolerate a range of positions for the stereocenter so the umbrella-like orientation can be catalytically productive and therefore must be included in explanations of enantioselectivity.
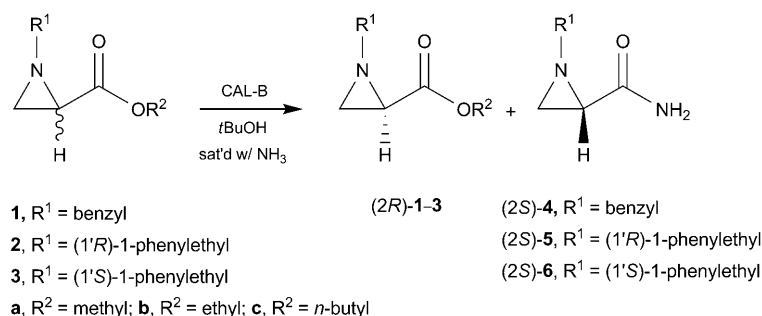
The CAL-B-catalyzed resolution discussed in this paper—like all other lipase-catalyzed resolutions—only preserves an existing stereocenter. Molecular modeling indicates that the N-alkyl aziridine-2-carboxylates cannot adopt an exchange-of-substituent orientation due to a combination of sterics and the rigid ring structure and an umbrella-like inversion orientation is the only way to rationalize the experimental results.

Results

1-Benzyl aziridine-2-carboxylates, 1 a–c

Initial screening of several lipases for their ability to catalyze the ammoniolysis of ethyl 1-benzyl aziridine-2-carboxylate (**1 b**) in tBuOH saturated with NH$_3$ identified CAL-B as the most promising enzyme. While lipases AYL (Amano AY from *Candida* sp.), CCL, PPL, and PSL (Amano PS from *Pseudomonas* sp.) showed < 20 % conversion after 20 h (data not shown), CAL-B showed 51 % conversion after only 0.8 h (Scheme 1, Table 1). HPLC analysis of the CAL-B-catalyzed reaction revealed an enantiomeric excess (*ee*) of 62 % for the unreacted ethyl ester and 56 % for the product amide; this corresponds to a moderate enantioselectivity of 7 ± 2 (Table 1, entry 2).

Chemical correlation established the absolute configuration of the enantiomer favored by CAL-B as (2S)-**1 b**. This chemical correlation involved converting the unreacted ester **1 b** to tBoc-alaninol (**7**), the absolute configuration of which is known. The conversion is analogous to the one in Scheme 2. Unreacted ester **1 b** (94 % *ee*; obtained after 85 % conversion and corresponding to E = 4) was reduced with LiAlH$_4$ followed

1, R^1 = benzyl
2, R^1 = (1′R)-1-phenylethyl
3, R^1 = (1′S)-1-phenylethyl
a, R^2 = methyl; **b,** R^2 = ethyl; **c,** R^2 = n-butyl

(2R)-**1–3**
(2S)-**4,** R^1 = benzyl
(2S)-**5,** R^1 = (1′R)-1-phenylethyl
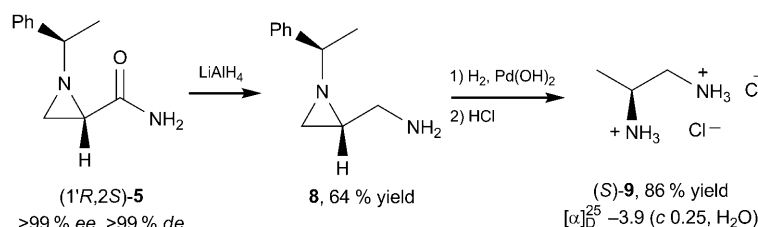(2S)-**6,** R^1 = (1′S)-1-phenylethyl

Scheme 1. CAL-B-catalyzed ammoniolysis of N-substituted aziridine carboxylates.

Table 1. CAL-B-catalyzed ammoniolysis of alkyl azirdine-2-carboxylates (**1–3**).

	Substrate[a]	R[1]	R[2]	t [h]	c[b] [%]	ee or de [%] ester[c]	amide[c]	E or D[d]
1	**1a**	PhCH₂	Me	1.0	55	73 (R)	31 (S)	6±3
2	**1b**	PhCH₂	Et	0.8	51	62 (R)	56 (S)	7±2
3	**1c**	PhCH₂	n-Bu	1.6	58	72 (R)	42 (S)	5±2
4	**2a**	(R)-PhCHMe	Me	1.3	56	>99 (1′R,2R)	>99 (1′R,2S)	>50
5	**2b**	(R)-PhCHMe	Et	2.1	56	>99 (1′R,2R)	>99 (1′R,2S)	>50
6	**2c**	(R)-PhCHMe	n-Bu	2.7	57	>99 (1′R,2R)	>99 (1′R,2S)	>50
7	**3a**	(S)-PhCHMe	Me	24	46	95 (1′S,2R)	97 (1′S,2S)	>50
8	**3b**	(S)-PhCHMe	Et	26	45	94 (1′S,2R)	>99 (1′S,2S)	>50

[a] The starting diastereomeric ratios of **2** and **3** were 44(1′R,2R):56(1′R,2S) and 56(1′S,2R):44(1′S,2S), respectively. [b] Conversion was determined by HPLC or GC with 2-bromonaphthalene as an internal standard. [c] The enantiomeric excess (ee) of esters and amides for substrate **1** were determined by chiral HPLC by using a Chiracel-ODH column. The diastereomeric excess (de) of esters and amides for substrates **2** and **3** were determined by capillary GC by using a Beta-DEX™ 120 column. [d] The enantioselectivity (E) or diastereoselectivity (D) was calculated according to C. S. Chen et al.[23] For **2a–c** and **3a–b**, we accounted for unequal amounts of the starting diastereomers.

duction of a sample of the product carboxamide **5** with LiAlH₄ followed by hydrogenolysis catalyzed by palladium yielded 1,2-diaminopropane dihydrochloride with $[\alpha]_D^{25}$ −3.9 (c 0.25, H₂O), which corresponds to the S configuration.[10]

1-((1′S)-1′-Phenylethyl)aziridine-2-carboxylates, 3a,b

The CAL-B-catalyzed ammoniolysis of methyl and ethyl (1-(1′S)-α-methylbenzyl)azirdne-2-carboxylate (**3a** and **b**) was also highly enantioselective (D > 50) and favored the 2S configuration, as above, but was approximately tenfold slower (Table 1, entries 7 and 8). Chemical preparation of **3a** and **3b** yielded a 56:44 ratio of 1′S,2R and 1′S,2S diastereomers, so the 45–46% conversion corresponds to complete ammoniolysis of the fast-reacting diastereomer. The diastereomeric purity of the remaining esters (95 and 94% de) and product amides (97 and >99% de) were slightly lower than for **2a–c**, but the diastereoselectivity of the reaction was still high, D > 50. Ammoniolysis of **3a** and **b** required 24–26 h to convert all of the fast-reacting diastereomer, while ammoniolysis of **2a–c** required only 1.3–2.7 h. Ammoniolysis of **1a–c** was slightly faster and required only 0.8–1.6 h to reach approximately 50% conversion.

Scheme 2. Chemical correlation established the 2S absolute configuration for the product carboxamide **5** from the CAL-B-catalyzed ammoniolysis of esters **2a–c**.

by hydrogenolysis in the presence of (Boc)₂O to yield tBoc-alaninol (**7**) with the $[\alpha]_D^{22}$ +10.1 (c 1.3, CHCl₃), which corresponds to the 2R configuration.[9] Thus, the favored enantiomer of **1b** had the 2S configuration. The enantioselectivity and rates were similar upon changing the alcohol portion of the ester from ethyl to methyl (**1a**) or n-butyl (**1c**; entries 1 and 3).

1-((1′R)-1′-phenylethyl)aziridine-2-carboxylates, 2a–c

The stereoselectivity of the CAL-B-catalyzed ammoniolysis increased significantly to D > 50 upon replacement of the N-benzyl substituent in the substrate with N-(1′R)-1′-phenylethyl (Table 1, entries 4–6). The structural difference between substrates **1** and **2** is small: **2** contains only an added methyl substituent at the methylene of the benzyl group.

Chemical preparation of alkyl aziridine-2-carboxylates from (R)-1-phenylethylamine and the corresponding alkyl 1,3-dibromopropionate yielded a 44:56 ratio of the 1′R,2R and 1′R,2S diastereomers for **2a–c**. The CAL-B-catalyzed ammoniolysis of this mixture completely separated the diastereomers. Both the product amide (**5**, 56% yield, 1′R,2S) and the unreacted ester (**2a–c**, 44% yield, 1′R,2R) showed >99% de. Reaction times for ammoniolysis of **2a–c** were similar to those for **1a–c**.

Chemical correlation established the favored diastereomer of **2a–c** as 2S (Scheme 2), which is the same as for **1a–c**. Re-

Molecular modeling approach

We used molecular modeling to propose a molecular basis for three of the experimental findings: 1) the tenfold lower rate of ammoniolysis for (2S)-**3a** as compared to (2S)-**1a** or −**2a**, 2) the enantiopreference of CAL-B for the 2S configuration of the aziridine carboxylate, and 3) the increased stereoselectivity when the N-alkyl group contains a methyl substituent. Starting from an X-ray crystal structure of CAL-B with a bound achiral phosphonate transition state analogue,[11] we modified it to correspond to the phosphonate transition state analogue for hydrolysis of methyl propanoate. We optimized the geometry of this analogue using molecular mechanics (consistent valence force field, CVFF, see Experimental Section for details) and verified that it adopted a catalytically productive conformation (Table 2, entry 1). Catalytically productive conformations were those that avoided steric clashes with the enzyme while maintaining the six catalytically essential hydrogen bonds (O/O or O/N distances < 3.0 Å and hydrogen bond angles ≥ 120°).

Next the propanoate was modified to the N-alkyl aziridines **1–3a**. These more complex structures contain four rotatable bonds. To find the best conformations, we systematically tried
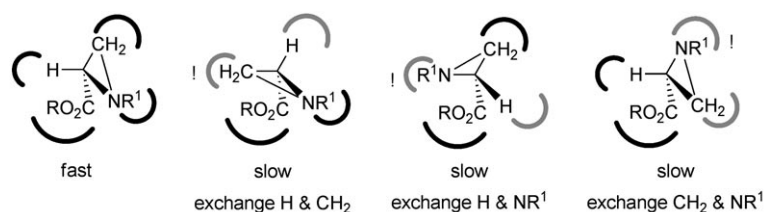
Table 2. Catalytically essential hydrogen bond measurements for selected modeled conformations.[a]							
	Substrate	H1	H2	H3	H4	H5	H6
1	methyl propanoate	2.81 (150°)	2.92 (152°)	3.01 (137°)	2.87 (160°)	2.52 (174°)	3.01 (137°)
2	(2S)-**1a**	2.82 (151°)	2.87 (153°)	3.00 (137°)	2.86 (161°)	2.50 (171°)	2.96 (172°)
3	(2R)-**1a**	2.84 (150°)	**3.09** (158°)	**3.07** (137°)	2.71 (165°)	2.58 (172°)	2.87 (170°)
4	(2S,1′R)-**2a**	2.81 (152°)	2.90 (148°)	2.93 (140°)	2.78 (162°)	2.54 (171°)	3.00 (174°)
5	(2R,1′R)-**2a**	2.85 (149°)	2.89 (163°)	**3.33** (135°)	2.69 (166°)	2.68 (171°)	2.92 (167°)
6	(2S,1′S)-**3a**	2.83 (151°)	2.88 (151°)	**3.07** (139°)	2.85 (160°)	2.51 (172°)	**3.03** (172°)
7	(2R,1′S)-**3a**	2.87 (149°)	**3.16** (156°)	**3.10** (139°)	2.65 (167°)	2.64 (171°)	2.86 (170°)

[a] The hydrogen bonds are defined in the Experimental Section (Scheme 5). The first number is the distance in Ångströms between the O or N atoms. A distance of >3.0 Å (marked in bold) suggests an inadequate hydrogen bond and a catalytically unproductive model. The number in parentheses is the X-H-X angle, where X is an O or N atom. The best orientation for hydrogen bond is linear (180°), but angles >120° suggest a hydrogen bond.

different orientations along these bonds (see Experimental Section for details). The geometry optimization procedure allowed both the backbone and side chains of the entire protein to move. This approach accounts for local protein flexibility and makes the modeling more realistic than a docking approach that uses a rigid enzyme.

This approach found a catalytically productive structure for each of the substrates that reacted quickly (both enantiomers of **1a** and the fast-reacting enantiomers of **2a** and **3a**; Table 2). In some cases, several rotamers yielded productive structures, but converged to similar structures upon further minimization. The slow reacting diastereomers of **2a** and **3a** did not yield catalytically productive conformations, but yielded several unproductive energy minima. For comparison, we chose structures for the slow reacting diastereomers of **2a** and **3a** that resembled the orientation of the slow-reacting enantiomer of **1a** (Table 2). In all cases the phenyl ring pointed toward the solvent; the shape of the active site prevented it from pointing inside the lipase.

None of the enantiomer pairs correspond to the current paradigm for enantioselectivity, that the relative orientation of enantiomers in a site are exchange-of-substituent positions (Scheme 3). Since the reaction center must remain at the active site serine, there are three possible exchange-of-substituent orientations. The three-membered ring limits the range of subtle adjustments for each of these three orientations. In each case, predicted steric interactions make the exchange-of-substituents orientation unlikely. For example, the only space available for the large *N*-alkyl substituent is in the site that it occupies in the fast enantiomer because this site is open in the direction of solvent. For this reason the last two structure in Scheme 3 are unrealistic. The only possible exchange of substituents is an exchange between the methylene and hydrogen substituents as in the second structure. Howev-

er, steric strain with active site wall (Ile189) prevented this orientation as well. In addition, these orientations cannot explain the three key experimental findings: 1) the tenfold lower rate of ammoniolysis for (2S)-**3a** as compared to (2S)-**1a** or -**2a**, 2) the enantiopreference of CAL-B for the 2S configuration of the aziridine carboxylate, and 3) the increased stereoselectivity when the *N*-alkyl group contains a methyl substituent.

Instead, the slow enantiomer adopts an umbrella-like inversion orientation (Scheme 4). In this orientation, the hydrogen substituent is in a different position, but the other three substituents are in the same sites.

Scheme 3. Schematic representation of the fast-reacting enantiomer of aziridine-2-carboxylate (2S, left) and three possible exchange-of-substituents orientations for the slow enantiomer (2R, right three structures). The curved lines represent the active site; gray curves indicate the two positions that have mismatched substituents for the slow enantiomer. The exclamation points indicate the regions where steric interactions make these orientations impossible.
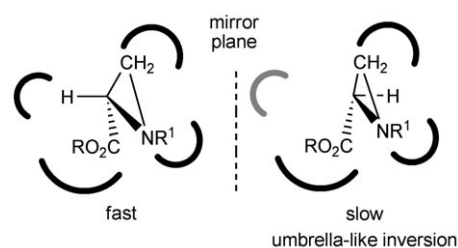
Scheme 4. Schematic representation of the fast-reacting enantiomer of aziridine-2-carboxylate (2S, left) and an umbrella-like inversion orientation of the slow enantiomer (2R, right) in the same site. The curved lines represent the active site, which are the same in both diagrams. The mirror plane shown relates the two molecules. This reflection places the hydrogen substituent of the slow enantiomer in a new location and leaves the original site empty (gray curve).

Slow reaction of (2S)-3 as compared to (2S)-1 and -2

Modeling suggests that a steric clash accounts for the approximately tenfold slower reaction of the (1′S)-1-phenylethyl compound, (2S)-**3a**, as compared to the benzyl compound, (2S)-**1a**

or (1'*R*)-1-phenylethyl compound, (2*S*)-**2a**. The 1'-methyl group of (2*S*)-**3a** clashes with the side chains of Ile189 and Thr138 in the active site (Figure 2). Several nonbonded hydrogen–hydrogen distances are near or below 2.0 Å, which we assumed indicates steric strain. (The van der Waals radius for a hydrogen

(2*S*,1'*R*)-**2a** fast　　　(2*S*,1'*S*)-**3a** slow
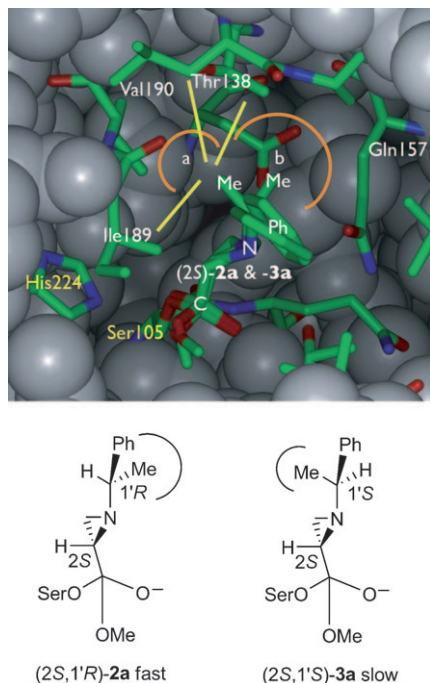
Figure 2. The active site of CAL-B fits the tetrahedral intermediate for hydrolysis of (2*S*,1'*R*)-**2a** better than that for (2*S*,1'*S*)-**3a**. Selected residues and the tetrahedral intermediates are shown as sticks, atoms in the rest of the lipase are shown as balls. Residues His224 and Ser105 (yellow labels) are part of the catalytic triad. The tetrahedral intermediates are covalently linked to Oγ of Ser105. The reaction center carbon (C), aziridine nitrogen (N) and phenyl group (Ph) occupy similar locations, but the 1'-methyl groups (Me) lie in different locations. For (2*S*,1'*S*)-**3a**, the 1'-methyl group points to the smaller region marked "a" and bumps into the side chain of several amino acids. The hydrogen–hydrogen contacts shown as yellow lines correspond to H–H distances of 1.99, 2.06 and 2.13 Å. For (2*S*,1'*R*)-**2a**, the 1'-methyl group points to the larger region marked "b". The only close contact is 2.07 Å to the side chain of Gln157. The scheme shows the two tetrahedral intermediates separately.

atom is 1.2 Å, but neutron diffraction data show nonbonded H–H distance as close as 2.0 Å.[12]) In contrast, the 1'-methyl of the (2*S*)-**2a** points in the opposite direction and fits comfortably between Gln157 and Thr138. The only close contact is 2.07 Å to the side chain of Gln157. The (2*S*)-**1a** lacks a 1'-methyl group and also fits in the active site (not shown). One can imagine two pockets at this point in the active site of CAL-B: a smaller one to the left, not quite big enough for a methyl substituent, and a larger one to right that can accommodate a methyl group. The hydrogen bond pattern is also consistent with steric strain for the (2*S*)-**3a** model. The slow reacting compound (2*S*)-**3a** shows a slightly longer distance of 3.09 Å between the serine oxygen and the histidine (Table 2, entry 6) while all hydrogen-bond distances are ≤ 3.0 Å for the fast reacting compounds (2*S*)-**1a** and (2*S*)-**2a** (entries 2 and 4). This

explanation for relative reactivity relies on the exchange-of-substituents paradigm. The methyl and hydrogen substituents at the 1'-position have exchanged positions.

Enantiopreference for the 2*S* over 2*R* configuration

The geometry-optimized tetrahedral intermediates for the (2*S*)- and (2*R*)-aziridine substrates adopt umbrella-like orientations in the actives site. Three of the substituents at the stereocenter (methylene, nitrogen and reaction center) lie in similar locations in the active site, while the hydrogen at the stereocenter points in opposite directions (Figure 3). This opposite orientation of this methine hydrogen can rationalize the observed
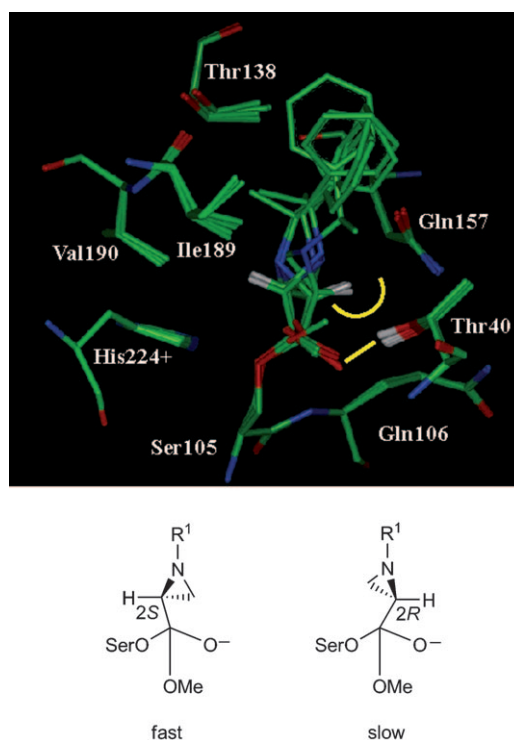

fast　　　slow

Figure 3. Orientation of the tetrahedral intermediates for the fast- and slow-reacting enantiomers of *N*-alkyl aziridine-2-carboxylates **1a**–**3a** in the active site of CAL-B. Superposition of the modeled tetrahedral intermediates and selected active site residues for the fast and slow enantiomers of **1a**–**3a**. The methine hydrogen of the three slow reacting substrates 2*R* clash (yellow semicircle) with the catalytically essential hydrogen bond (yellow line between Oγ of Thr40 and the oxyanion oxygen). The scheme shows the umbrella-like relative orientation of the enantiomers.

enantiopreference. For the fast-reacting 2*S* configuration, the methine hydrogen points away from Thr40 Oγ hydrogen. For the slow reacting 2*R* configuration this methine hydrogen stands close (2.12, 1.99 and 2.10 Å) to the Thr40 Oγ hydrogen, which makes a catalytically essential hydrogen bond, H5. We hypothesize that this H–H clash slows reaction of the 2*R* substrates. The hydrogen bond distance between Thr40 Oγ and the oxyanion oxygen is indeed ~0.1 Å longer in the 2*R* structures as compared to the 2*S* structures in Table 2, but the hy-

drogen bond is maintained in all structures. Magnusson and co-workers showed that breaking this hydrogen bond in CAL-B slows the reaction.[13]

In the umbrella-like inversion orientation, the alkyl chains of both enantiomers bind to the wide binding site in CAL-B. Although this site is wide, adding a methyl group causes structural adjustments that can account for the tenfold increase in enantioselectivity. We propose that the extra methyl group in the *N*-phenylethyl aziridines as compared to the *N*-benzyl aziridines increases enantioselectivity by structural adjustments that weaken or break hydrogen bonds H2 or H3 (His224 to either the alcohol oxygen or the Ser105 Oγ; Table 2). The slow enantiomer for the *N*-benzyl aziridine shows slightly longer H2 and H3 bonds than the fast enantiomer (compare entries 2 and 3). However, for the slow reacting diastereomer of the *N*-phenylethyl aziridines, one or both hydrogen bonds are broken (N–O distance $\geq$ 3.1 Å; compare entries 4 with 5 and 6 with 7). This breaking is caused by structural adjustments of the tetrahedral intermediate to accommodate the extra methyl group. For the (2*R*)-**2a** model, the α-methyl group cannot fit in the acyl binding pocket and turns to face the alcohol-binding pocket; this disrupts hydrogen bonds to His224 (entry 5). For the (2*R*)-**3a** model, the 1′-methyl sits in the acyl-binding pocket ("a" region). However, it clashes with nearby amino acids, with H–H contact distances of 2.09 and 2.12 Å to Thr138 and 2.15 Å to Ile189; this likewise disrupts hydrogen bonds to His224 (entry 7).

Discussion

Adding a (*R*)- or (*S*)-1′-methylbenzyl group to racemic 2-aziridine carboxylates creates diastereomers. Although chromatography can separate these diastereomers, it is not suitable for multikilogram synthesis. The CAL-B-catalyzed ammoniolysis converts the 2*S* diastereomer to the carboxamide. Partitioning between *n*-hexane and water separates the unreacted (2*R*)-aziridine-2-carboxylate ester (*n*-hexane soluble) and (2*S*)-aziridine-2-carboxamide (water soluble) without resorting to chromatographic separation. The ease of obtaining chiral aziridine-2-carboxylates through this lipase-mediated reaction should spur other applications for this synthon. The (*R*)- or (*S*)-methylbenzyl substituent not only increases the enantioselectivity of CAL-B as compared to the benzyl substituent, but also increases the stereoselectivity for several subsequent reactions (e.g., ~2.7-fold for dihydroxylation[14]). Hydrogenolysis or metal-ammonia reduction can remove the (*R*)- or (*S*)-methylbenzyl substituent.[15]

For CAL-B-catalyzed reactions of secondary alcohols, the classical paradigm of exchange-of-substituents works well. The substituents bind in the large pocket and medium pocket (also called the stereoselectivity pocket) that form the alcohol-binding site. The slow enantiomer can adopt a catalytically productive orientation when the medium and large substituents bind in the incorrect pockets, and this exchange-of-substituent orientation can account for changes in enantioselectivity.[16] The umbrella-like orientation of several secondary alcohols in CAL-B did not appear to be catalytically productive. In contrast, we find a different molecular basis for the enantioselectivity of CAL-B toward chiral acids, such as the *N*-alkyl aziridine-2-carboxylates.

The reactivity and selectivity depend on the orientation of a stereocenter that is far (three bonds away) from the reaction site. Several other groups have reported lipase-catalyzed enantioselective reactions of chiral acids containing remote stereocenters,[17] but did not suggest a molecular basis for enantioselectivity. One problem with modeling of substrates with remote stereocenters is the large number of possible conformations to consider. The rigid three-membered aziridine ring limits the number of conformations available to compounds **1a**–**3a** in the active site. This limitation simplified the modeling for this case.

The slightly larger space on one side of the active site of CAL-B can explain the tenfold-lower reactivity of substrates with an *N*-(1′*S*)-phenethyl substituent over the *N*-(1′*R*)-phenethyl and *N*-benzyl substituents. The methyl group in the 2*S*,1′*R* substrate bumps into the active site wall, while for the 2*S*,1′*S* substrate the methyl group points to the larger space. The *N*-benzyl group lacks the methyl substituents and thus encounters no hindrance.

The relative orientation of enantiomeric aziridine rings differs from the classical paradigm to explain enantioselectivity. The enantiomeric aziridine rings adopt an umbrella-like-inversion orientation. The carboxyl carbon, methylene and aziridine nitrogen lie in similar location for both enantiomers. The two stereocenters are displaced and the methine hydrogens point in opposite directions.

The relative orientation of the enantiomeric aziridine rings leads to a different explanation for enantioselectivity. If the slow enantiomer reacts through an orientation that switches two substituents, then enantioselectivity relies on distinguishing those two substituents. This is the most common approach to explain enantioselectivity. If the slow enantiomer reacts through an umbrella-like-inversion orientation, then the enantioselectivity relies on distinguishing the different hydrogen orientations. In this case, for the fast-reacting enantiomer, this methine hydrogen lies out of the way. For the slow-reacting enantiomer, this methine hydrogen appears to bump a key residue in the oxyanion hole. This bumping distorts the orientation of the tetrahedral intermediate, and thus breaks catalytically essential hydrogen bonds. Enantioselectivity also involves distinguishing subtle differences in the orientations of the three other substituents. The higher enantioselectivity of the *N*-phenylethyl-substituted aziridines over the *N*-benzyl aziridines is due to differences in the orientations of these substituents, which all bind in approximately the same region.

Several researchers have previously considered the role of umbrella-like binding in the enantioselectivity of enzymes.[5, 8, 18, 19] This is the first attempt to use it in modeling to explain the detailed molecular basis for enantioselectivity. The example involves chiral acyl compounds, which often adopt an umbrella-like orientation. In the previous review of enantiomers bound to enzymes and proteins, we identified sixteen examples of enantiomers bound in an umbrella-like orientation.[8] Of these sixteen, seven were carboxylic acids and four were

boronate analogues of carboxylic acids. Because of the prevalence of chiral acyl compounds in these examples, we feel it is especially important to consider the umbrella-like binding mode for explanations of enantioselectivity toward chiral acyl compounds, but that umbrella-like binding might contribute to the enantioselectivity of any chiral compound in which the stereocenter is not the reaction site.

Conclusions

CAL-B-catalyzed ammoniolysis of aziridine-2-carboxylates (**2**) is highly enantioselective and is a convenient route to enantiopure material. The classical paradigm for enantioselectivity—enantiomers binding in an exchange-of-substituents orientation—could not explain the experimental results. The rigid substrate and narrow active site limited the possible orientations of the substrate and did not allow the enantiomer to bind in an exchange-of-substituents fashion. Another relative orientation of enantiomers—an umbrella-like orientation—could rationalize the enantioselectivity due to different orientations of the methine hydrogen in the two enantiomers. This new paradigm for enantioselectivity should be considered for all reactions that occur near a stereocenter, such as lipase-catalyzed reactions.

Experimental Section

General: NMR spectra were recorded in CDCl$_3$ unless otherwise noted at 200 MHz (^{1}H) or 50.3 MHz (^{13}C); chemical shifts are in ppm. Melting points are uncorrected. Optical rotations were measured by using concentrations "*c*" in g pe 100 mL in the solvents indicated. Commercially available reagents were from Aldrich or Fluka, and were used without purification. Analytical thin layer chromatography on precoated silica gel glass plates (Merck Kieselgel 60F254 layer thickness 0.2 mm) were eluted with *n*-hexane/EtOAc (3:1) unless otherwise noted and visualized with a UV lamp (254 nm), phosphomolybric acid, or ninhydrin. Column chromatography was conducted with silica gel grade 200–300 mesh. Anhydrous procedures were performed under a nitrogen atmosphere with purified solvents, oven-dried syringes stored in a descicator and oven-dried glassware. Immobilized *Candida antarctica* lipase B (CAL-B, Chirazyme L-2, c.-f., lyo; Boehringer Mannheim), lipase PS "Amano" LPSAU11529 (PSL, Amano Pharmaceutical, Co.), lipase AY "Amano" 30 LAYU10515 (AYL, Amano Pharmaceutical, Co.), porcine pancreas lipase (PPL, Sigma) and lipase from *Candida cylindracea* (CCL, also known as *Candida rugosa*; Sigma) were used as received.

Alkyl aziridine-2-carboxylates: Solid Na$_2$CO$_3$ (3 equiv) and the corresponding amine (RNH$_2$, 1.5 equiv, benzylamine for **1**, (*R*)-1-phenylethylamine for **2**, and (*S*)-1-phenylethylamine for **3**) were added to a solution of alkyl dibromopropionate in acetonitrile and the mixture was stirred at room temperature for 20 h. Na$_2$CO$_3$ was filtered off and the reaction solution was extracted with CH$_2$Cl$_2$ and brine. The organic layer was separated and the aqueous layer was extracted with CH$_2$Cl$_2$. The combined organic layers were dried over anhydrous MgSO$_4$, filtered and evaporated in vacuo. The resulting yellow oil of **1** was purified by short path column chromatograph. Substrates **2** and **3** were used as diastereomeric mixtures without further purification. Spectroscopic data for compounds **2** and **3** were reported previously.[6]

Methyl 1-benzylaziridine-2-carboxylate, (±)-1a: Yield: 71%; R_f= 0.22; ^{1}H NMR: δ = 7.33–7.27 (m, 5H), 3.70 (s, 3H), 3.52 (s, 2H), 2.25–2.19 (m, 2H), 1.74 (d, *J*=6.6 Hz, 1H); ^{13}C NMR: δ = 171.0, 137.5, 128.2, 127.9, 127.2, 63.7, 52.1, 37.1, 34.4.

Ethyl 1-benzylaziridine-2-carboxylate, (±)-1b: Yield: 98%; R_f= 0.28; ^{1}H NMR: δ = 7.31–7.27 (m, 5H), 4.24–4.10 (m, 2H), 3.52 (s, 2H), 2.23–2.14 (m, 2H), 1.72 (dd, *J*=5.0, 1.4 Hz, 1H), 1.24 (t, *J*= 7.2 Hz, 3H); ^{13}C NMR: δ = 170.5, 137.5, 128.1, 127.7, 127.0, 63.5, 60.8, 37.2, 34.2, 13.9.

***n*-Butyl 1-benzylaziridine-2-carboxylate, (±)-1c**: Yield: 81%; R_f= 0.34; ^{1}H NMR: δ = 7.28–7.22 (m, 5H), 4.14–4.00 (m, 2H), 3.49 (m, 2H), 2.15 (m, 2H), 1.67 (m, 1H), 1.56 (m, 2H), 1.30 (m, 2H), 0.86 (t, *J*=6.2 Hz, 3H); ^{13}C NMR: δ = 170.4, 137.5, 127.9, 127.5, 126.8, 64.5, 63.3, 37.0, 34.1, 30.1, 18.6, 13.3.

CAL-B-catalyzed ammoniolysis of alkyl aziridine-2-carboxylates 1–3: *tert*-Butyl alcohol was saturated with ammonia by bubbling the gas through the dried solvent for approximately 1 h. CAL-B (50 mg) and 2-bromonaphthalene (0.24 mmol, 50 mg, internal standard) were added to a solution of aziridine ester (approximately 1.2 mmol) in *tert*-butyl alcohol saturated with ammonia (5.0 mL) in a two-neck round-bottom flask (25 mL) and stirred at 35 °C. To monitor the progress of the reaction, aliquots (50 µL) of the reaction mixture were diluted with ethanol (1.5 mL) and analyzed by GC and/or HPLC. At the desired conversion, the reaction was stopped by filtering off the lipase. The immobilized lipase was washed with methanol and the combined organic filtrates were concentrated in vacuo. The residue was dissolved in water (3 mL) and *n*-hexane (10 mL) and the layers were separated. The combined organic layer were dried over MgSO$_4$, filtered and concentrated in vacuo. For synthesis purposes, the above procedure was scaled up and the 2-bromonaphthalene internal standard was omitted. The conversion and diastereomeric or enantiomeric excess of esters **1**–**3** and amides **4**–**6** were determined by capillary GC by using Beta-DEX™ 120 column (Supelco); injection temp: 220 °C, detection temp: 230 °C, flame ionization detector, 0.5 µL sample size, flow rate 1.22 mL min^{-1} of N$_2$ with 20 psi. Retention times of amides **4**–**6**: 18–20 min (2*S* configuration), 21–23 min (2*R* configuration); esters **1**–**3**: 30–31 min (2*S* configuration), 32–33 min (2*R* configuration).

Ethyl 1-benylaziridine-(2*R*)-carboxylate. (*R*)-1b: CAL-B (650 mg) catalyzed ammoniolysis of **1b** (3.23 g, 15.8 mmol) to 79% conversion yielded the unreacted ester with 94% *ee*; $[\alpha]_D^{25}$ +61 (*c* 4.5, CH$_2$Cl$_2$).

1-Benzylaziridine-(2*S*)-carboxamide, (*S*)-4: R_f=0.05; m.p. 102–104 °C; ^{1}H NMR (CD$_3$OD): δ = 7.24–7.18 (m, 5H), 3.40 (m, 2H), 2.08 (dd, *J*=2.7, 6.5 Hz, 1H), 1.71 (d, *J*=6.6 Hz, 2H); ^{13}C NMR (CD$_3$OD): δ = 175.6, 139.5, 129.4, 129.1, 128.3, 63.9, 39.6, 35.3; MS *m/z* (%) 176 ([*M*]$^+$, 0.09), 175 (0.7), 159 (2), 130 (8), 104 (17), 91 (100), 77 (9), 72 (12), 65 (13), 51 (9); elemental analysis calcd (%) for C$_{10}$H$_{12}$N$_2$O: C 68.7, H 6.86, N 15.9; found: C 68.4, H 6.61, N 15.7.

Methyl 1-((1′*R*)-1′-phenylethyl)-aziridine-(2*R*)-carboxylate, (1′*R*,2*R*)-2a: Yield 98%; R_f=0.43; ^{1}H NMR: δ = 7.41–7.22 (m, 5H), 3.75 (s, 3H), 2.54 (q, *J*=6.6 Hz, 1H), 2.22 (dd, *J*=6.2, 3.1 Hz, 1H), 2.13 (dd, *J*=3.2, 1.4 Hz, 1H), 1.61 (dd, *J*=6.6, 1.0 Hz, 1H), 1.47 (d, *J*=6.6 Hz, 3H); ^{13}C NMR: δ = 171.2, 143.2, 128.2, 127.2, 126.7, 69.8, 52.2, 38.0, 33.9, 23.0.

Ethyl 1-((1′*R*)-1′-phenylethyl)-aziridine-(2*R*)-carboxylate, (1′*R*,2*R*)-2b: Yield 98%; R_f=0.68; ^{1}H NMR: δ = 7.41–7.22 (m, 5H), 4.31–4.10 (m, 2H), 2.54 (q, *J*=6.6 Hz, 1H), 2.47 (dd, *J*=6.2, 3.0 Hz, 1H), 2.13 (dd, *J*=6.2, 3.0 Hz, 1H), 1.57 (dd, *J*=6.4, 1.0 Hz, 1H), 1.48 (d, *J*=

6.6 Hz, 3H), 1.30 (t, $J = 7.2$ Hz, 3H); ^{13}C NMR: $\delta = 170.9$, 143.4, 128.3, 127.2, 126.8, 69.9, 61.1, 38.1, 33.9, 23.1, 14.1.

n-Butyl 1-((1′R)-1′-phenylethyl)-aziridine-(2R)-carboxylate, (1′R,2R)-2c: Yield 98%; $R_f = 0.60$; ^{1}H NMR: $\delta = 7.42$–7.22 (m, 5H), 4.28–4.06 (m, 2H), 2.53 (q, $J = 6.6$ Hz, 1H), 2.32 (m, 1H), 2.22 (m, 2H), 1.68 (m, 2H), 1.48 (d, $J = 5.6$ Hz, 3H), 1.46 (m, 2H), 0.95 (t, $J = 6.6$ Hz, 3H); ^{13}C NMR: $\delta = 170.7$, 143.2, 128.1, 127.0, 126.6, 69.6, 64.7, 37.9, 33.7, 30.4, 23.0, 18.8, 13.51.

1-((1′R)-1′-phenylethyl)-aziridine-(2S)-carboxamide, 5: $R_f = 0.27$ (EtOAc); $[\alpha]_D^{25} = -32.4$ (c 0.8, CH$_3$OH); m.p. 98–100 °C; ^{1}H NMR (CD$_3$OD): $\delta = 7.29$–7.10 (m, 5H), 2.52 (q, $J = 6.4$ Hz, 1H), 2.00 (d, $J = 2.6$ Hz, 1H), 1.90 (dd, $J = 2.8$, 6.6 Hz, 1H), 1.73 (d, $J = 7.0$ Hz, 1H), 1.28 (d, $J = 6.4$ Hz, 3H); ^{13}C NMR (CD$_3$OD): $\delta = 175.6$, 145.2, 129.4, 128.2, 127.6, 70.1, 39.0, 35.6, 23.6; MS m/z (%): 190 (0.13) $[M]^+$, 189 (1), 175 (3), 157 (2), 144 (7), 130 (4), 119 (3), 105 (100), 77 (18), 72 (5), 51 (7); elemental analysis calcd (%) for C$_{11}$H$_{14}$N$_2$O: C 69.5, H 7.42, N 14.7; found: C 69.4, H 7.71, N 14.7.

Methyl 1-((1′S)-1′-phenylethyl)-aziridine-(2R)-carboxylate, (1′S,2R)-3a: Yield 98%; $R_f = 0.23$; ^{1}H NMR: $\delta = 7.33$–7.20 (m, 5H), 3.62 (s, 3H), 2.53 (q, $J = 6.6$ Hz, 1H), 2.31 (dd, $J = .2$, 0.8 Hz, 1H), 2.04 (dd, $J = 6.8$, 3.0 Hz, 1H), 1.75 (dd, $J = 5.6$, 1.0 Hz, 1H), 1.43 (d, $J = 6.6$ Hz, 3H); ^{13}C NMR: $\delta = 170.8$, 143.4, 128.2, 127.0, 126.2, 69.5, 51.9, 36.7, 34.8, 23.3.

Ethyl 1-((1′S)-1′-phenylethyl)-aziridine-(2R)-carboxylate, (1′S,2R)-3b: Yield 98%; $R_f = 0.44$; ^{1}H NMR: $\delta = 7.36$–7.23 (m, 5H), 4.13 (q, $J = 7.2$ H, 2Hz), 2.56 (q, $J = 6.6$ Hz, 1H), 2.33 (dd, $J = 3.2$, 1.2 Hz, 1H), 2.04 (dd, $J = 6.6$, 3.2 Hz, 1H), 1.76 (dd, $J = 6.6$, 1.2 Hz, 1H), 1.45 (d, $J = 7.4$ Hz, 3H), 1.19 (t, $J = 7.2$ Hz, 3H); ^{13}C NMR: $\delta = 170.6$, 143.7, 128.4, 127.1, 126.4, 69.6, 60.9, 37.1, 34.8, 23.5, 14.1.

1-((1′S)-1′-phenylethyl)-aziridine-(2S)-carboxamide, 6: $R_f = 0.48$ (EtOAc 100%); $[\alpha]_D^{25} = -104$ (c 0.5, CH$_3$OH); m.p. 110–112 °C; ^{1}H NMR (CD$_3$OD): $\delta = 7.29$–7.10 (m, 5H), 2.50 (q, $J = 6.5$ Hz, 1H), 2.10 (dd, $J = 2.8$, 6.6 Hz, 1H), 1.75 (d, $J = 2.8$ Hz, 1H), 1.51 (d, $J = 6.6$ Hz, 1H), 1.29 (d, $J = 6.4$ Hz, 3H); ^{13}C NMR (CD$_3$OD): $\delta = 176.0$, 145.0, 129.4, 128.3, 127.9, 69.9, 40.0, 34.8, 23.4; MS m/z (%) 190 (0.07) $[M]^+$, 189 (0.8), 172 (1), 157 (2), 14 6(7), 131 (4), 119 (5), 105 (100), 77 (18), 72 (7), 51 (6); elemental analysis calcd (%) for C$_{11}$H$_{14}$N$_2$O: C 69.5, H 7.42; N 14.7; found: C 69.5, H 7.60, N 14.4.

Absolute configuration of 1b: LiAlH$_4$ (96.4 mg, 2.54 mmol) was added in portions to a dry THF solution (2.0 mL) of ethyl 1-benzyla-ziridine-(2R)-carboxylate (1b; 260 mg, 1.27 mmol) isolated from a CAL-B-catalyzed ammoniolysis under N$_2$ at 0 °C. After being stirred for 5 h, the reaction was quenched by the addition of saturated aqueous KHSO$_4$, filtered and the filtrate was evaporated in vacuo to afford 1-benzyl-(2R)-hydroxymethylaziridine as a white solid. Yield: 139 mg (67%); $R_f = 0.15$ (EtOAc); $[\alpha]_D^{25} = +13.3$ (c 1.75, CH$_2$Cl$_2$); m.p. 78–80 °C; ^{1}H NMR: $\delta = 7.26$–7.18 (m, 5H), 4.24 (br s, 1H), 3.66 (dd, $J = 11.5$, 3.1 Hz, 1H), 3.42 (d, $J = 13.2$ Hz, 1H), 3.25 (d, $J = 13.6$ Hz, 1H), 3.21 (d, $J = 12.2$ Hz, 1H), 1.80–1.72 (m, 1H), 1.37 (d, $J = 5.8$ Hz, 2H); ^{13}C NMR: $\delta = 138.5$, 128.3, 127.9, 127.1, 63.8, 62.4, 40.8, 30.8. A mixture of 1-benzyl-(2R)-hydroxymethylaziridine (138 mg, 0.845 mmol), Pd/C (10%; 14 mg) and (Boc)$_2$O (203 mg, 0.930 mmol) in CH$_3$OH (5.0 mL) were stirred under a balloon pressure of hydrogen for 18 h at room temperature. The catalyst was filtered off and the solution was dried in vacuo. The crude product was purified by silica gel column chromatography eluted with n-hexane/EtOAc (2:1) to afford N-tBoc-D-alaninol as a colorless oil. Yield: 115 mg (78%); $R_f = 0.15$ (n-hexane/EtOAc, 2:1); $[\alpha]_D^{25} = +10.1$ (c 1.3, CHCl$_3$); ^{1}H NMR: $\delta = 3.74$–3.58 (m, 1H), 3.52–3.40 (m, 2H),

1.43 (s, 9H), 1.13 (dd, $J = 6.6$, 1.2 Hz, 3H); ^{13}C NMR: $\delta = 156.2$, 79.5, 66.8, 48.4, 28.3, 17.2.

Absolute configuration of 5 (Scheme 2) and 6: LiAlH$_4$ (320 mg, 8.44 mmol) was added in portions to a dry DMF solution (20 mL) of 1-((1′R)-α-methylbenzyl)-aziridine-(2S)-carboxamide (5; 401 mg, 2.11 mmol, obtained from a CAL-B-catalyzed ammoniolysis) warmed to 55–60 °C and stirred for 20 h. The reaction was quenched by addition of a saturated KHSO$_4$ solution, filtered and the filtrate was evaporated in vacuo. The residue was purified by silica gel chromatography eluted with CH$_2$Cl$_2$/CH$_3$OH (2:1) to afford (2R)-aminomethyl-1-[(1′R)-1′-phenyethyl]aziridine (8) as pale yellow oil. Yield: 252 mg (64%); $R_f = 0.28$ (CH$_2$Cl$_2$/CH$_3$OH, 2:1); $[\alpha]_D^{25} = +65$ (c 0.90, CHCl$_3$); ^{1}H NMR: $\delta = 7.30$–7.05 (m, 5H), 2.59 (d, $J = 3.6$ Hz, 1H), 2.53 (d, $J = 4.0$ Hz, 1H), 2.26 (m, 1H), 2.29 (q, $J = 4.8$, 6.6 Hz, 1H), 1.63 (d, $J = 3.2$ Hz, 1H), 1.29 (d, $J = 6.6$ Hz, 3H), 1.22 (d, $J = 1.8$ Hz, 1H); ^{13}C NMR: $\delta = 144.2$, 127.8, 126.6, 126.2, 69.3, 44.1, 40.5, 31.8, 22.2. MS m/z (%) 176 ($[M]^+$, 0.4), 158 (21), 132 (23), 120 (11), 105 (100), 91 (15), 77 (37), 71 (25), 51 (14); elemental analysis calcd (%) for C$_{11}$H$_{16}$N$_2$: C 75.0, H 9.15, N 15.9; found: C 75.3, H 9.21, N 16.0. A mixture of 8 (142 mg, 0.81 mmol) in CH$_3$OH (4.0 mL) and 10% Pd(OH)$_2$ on carbon (14 mg) was stirred under hydrogen (5 bar) for 5 days at room temperature. The catalyst was filtered off and the solution was cooled below 10 °C in an ice bath. Dry HCl was bubbled slowly into the solution and stirred for 2 h. The solution was evaporated in vacuo to afford a white solid, which was recrystalized from CH$_3$OH/Et$_2$O to give (S)-(−)-1,2-diaminopropane dihydrochloride, (S)-9, as a white solid: 101 mg, 86%; $[\alpha]_D^{25} = -3.9$ (c 0.25, H$_2$O), literature value in ref. [10] $[\alpha]_D^{20} = -4$ (c 20, H$_2$O); $[\alpha]_D^{20} = -4$ (c 20, H$_2$O); m.p. 236–238 °C; ^{1}H NMR (D$_2$O): $\delta = 3.63$ (m, 1H), 3.18 (m, 2H), 1.31 (d, $J = 6.6$ Hz, 3H); ^{13}C NMR (D$_2$O): $\delta = 44.7$, 41.4, 15.2. The absolute configuration of 6 was determined by the same procedure with the formation of (S)-(−)-1,2-diaminopropane dihydrochloride: 72 mg, 86% yield, $[\alpha]_D^{25} = -4.0$ (c 0.37, H$_2$O).

Molecular modeling: Molecular modeling was performed by using Discover 2.9.7, in the Biosym MSI Insight II environment, version 97.0 (Biosym/MSI, San Diego, CA, USA) with the consistent valence force field (cvff),[20] which correctly reproduced the pyramidal configuration of the aziridine nitrogen atom.[21] The starting X-ray structure of *Candida antarctica* lipase B (PDB ID: 1lbs[11]) contained a bound phosphonate inhibitor. Hydrogen atoms were added to the X-ray structure to correspond to the protonation state at pH 7, except for the catalytic His224 residue, which was set to pH 4.5 in order to add a proton. The pK_a values of the amino acid side chain residues were taken to be the same as for the free amino acids and were not calculated. The positions of the added hydrogen atoms were optimized with 1000 iterations of energy minimization by using the steepest descent algorithm. The bound phosphonate inhibitor was modified to a tetrahedral intermediate corresponding to hydrolysis of methyl propanoate (Scheme 5). In this and subsequent steps, the partial charges of the tetrahedral intermediate were set according to a semiempirical MOPAC (MNDO) calculation. The water molecules were minimized with a steepest descent algorithm keeping the enzyme fixed. Next, both the side chains and the water molecules were minimized with the steepest descent algorithm, first for 1500 iterations with the atoms tethered to their starting position with a slight restoring force of 10 kcal Å^{-2} and next for 1000 iterations without constraints. Afterwards, the entire enzyme was minimized, with the steepest descent algorithm, first for 1500 steps with a tethering force of 25 kcal Å^{-2}, and then without any constraint. The enzyme was finally minimized with a conjugate gradient algorithm to a root mean square (RMS) derivative value of ≤ 0.001 Å mol^{-1}. The resulting tetrahedral intermediate

A)

B)
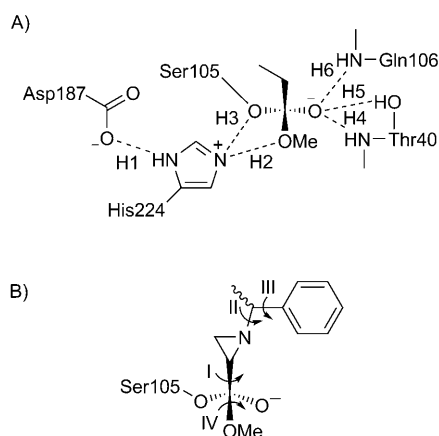
Scheme 5. Tetrahedral intermediates in the CAL-B-catalyzed hydrolysis of esters. A) Tetrahedral intermediate for hydrolysis of methyl propanoate. Six catalytically essential hydrogen bonds (H1–H6) form between the intermediate, the catalytic triad (Asp187, His224 and Ser105), and the oxyanion hole (Gln106, Thr40). Hydrogen bond lengths and angles for the optimized geometry of this intermediate are in Table 2. B) The tetrahedral intermediate for hydrolysis of methyl (1-phenylethyl)aziridine-2-carboxylate contains four rotatable bonds (I–IV). A systematic search of possible orientations of these bonds ensured that the best geometry for the intermediate was identified.

contained all key hydrogen bonds (Scheme 5 and Table 2) and was used for further modeling.

Conformational search: Conformations were generated by using a systematic rotor search about each of the four rotatable bonds (Scheme 4). First, from the bare tetrahedral intermediate, an unsubstituted aziridine ring was built for both the 2*R* and 2*S* substrates and the "Nearby" subset of amino acids enclosing the acyl binding site was defined. This subset comprised Thr40, Ser105, Gln106, Asp134, Thr138, Leu140, Ala141, Val154, Gln157, Ile189, Val190, Ile285, as well as His224+ and the tetrahedral intermediate. For both enantiomers, a rotor search for bond I was performed for a complete turn with 15° increments. After each increment, the Nearby subset of amino acids was minimized with 100 steps of steepest gradient to relax steric strain. Three minima for each enantiomer were selected from the potential energy profile and saved. A methyl group was added to the nitrogen atom of each of these minima and the Nearby subset of amino acids was left to minimize with a steepest descent followed with a conjugate gradient algorithm to a RMS derivative of 0.01 Åmol⁻¹. For each of these six structures, a phenyl group was added so as to form the 1-benzylaziridine-2-carboxylate tetrahedral intermediates. Two rotor searches were performed for bond II for a complete period, with increments of 15°. For bond III, the dihedral angle was set to 0° and 90° for each of the rotor searches for the second rotatable bond. It was assumed that minima between these two conformations would be established in subsequent minimizations. In order to generate an energy profile, the potential energy of Ser105 and the attached tetrahedral intermediate was recorded at every rotor increment. Structures corresponding to the minima of these energy profiles were kept for further analysis. Although bond IV rotates freely in solution, only a limited number of conformations in the active site are productive. Explicitly, one of the two oxygen lone pairs should be collinear with the catalytic histidine N−H bond. However, one such conformation would induce a 1,4-steric clash between the methyl group and the aziridine group. Hence, only the conformation with the methyl group *anti* to the aziridine group was retained. In the end, all of the structures obtained from

this systematic conformational search were set aside. A methyl group was added to the α-methyl of each of these substrates to generate the rotamers for the (2*S*,1′*S*), (2*S*,1′*R*), (2*R*,1′*S*) and (2*R*,1′*R*) compounds.

Geometry optimization: The geometry of the structures produced during the conformational search was optimized as follows. First, Ser105 and the attached tetrahedral intermediate were energy minimized individually for 1500 steps of steepest descent. Then, the whole Nearby set was left to minimize 5000 steps of steepest gradient, followed by conjugate descent minimization to a root-mean-square derivative of 0.01 Åmol⁻¹. These local minima were relaxed with molecular dynamic simulations. A short 5000 ps dynamic with a step size of 1 ps and a temperature of 300 K was performed on the Nearby set, and the history was sampled every 50 steps. Any significant conformational changes usually occurred in the first 500 ps. Afterwards, a structure with good hydrogen bonds and low in potential energy and which occurred after any significant conformational changes, was selected and further minimized. The 2000 steps of steepest-descent minimization were carried out on the Nearby set of amino acids, and minimization to a RMS of 0.01 with the conjugate gradient algorithm followed. These energy-minimized molecules were assessed for catalytic relevance.

Analysis of conformers: The catalytic triad of each modeled substrate was assessed in accordance with the charge relay model.[22] A catalytically productive conformation was one that formed all six hydrogen bonds in Scheme 5 A. A heteroatom–heteroatom distance of ≤ 3.00 Å indicated a strong hydrogen bond, a distance between 3.00 and 3.10 Å indicated a weak hydrogen bond and a distance > 3.10 Å indicated no hydrogen bond. The angle between the two heteroatoms and the hydrogen in the hydrogen bond should be close to 180°, but any angle ≥ 120° was considered to produce a hydrogen bond. Structures lacking one or more hydrogen bonds were deemed unproductive.

[1] G. Cardillo, L. Gentilucci, A. Tolomelli, *Aldrichimica Acta* **2003**, *36*, 39–50; M.-J. Suh, S. W. Kim, S. I. Beak, H.-J. Ha, W.-K. Lee, *Synlett* **2004**, 489–492; J. M. Yun, T. B. Sin, H. S. Hahm, W. K. Lee, H.-J. Ha, *J. Org. Chem.* **2003**, *68*, 7675–7680.

[2] Review: W.-K. Lee, H.-J. Ha, *Aldrichimica Acta* **2003**, *36*, 57–64; See also: W. K. Lee, C. S. Park, Y. H. Lim, H. J. Ha, US Patent, **2007**, 7 268 228.

[3] M. Martres, G. Gil, A. Méou, *Tetrahedron Lett.* **1994**, *35*, 8787–8790; H. M. Sampath Kumar, M. Shesha Rao, P. Pawan Chakravarthy, J. S. Yadav, *Tetrahedron: Asymmetry* **2004**, *15*, 127–130.

[4] Review: V. Gotor, *Bioorg. Med. Chem.* **1999**, *7*, 2189–2197.

[5] Review: R. Bentley, *Arch. Biochem. Biophys.* **2003**, *414*, 1–12.

[6] C. Orrenius, F. Haeffner, D. Rotticci, N. Ohrner, K. Hult, *Biocatal. Biotransform.* **1998**, *16*, 1–15.

[7] P. F. Mugford, U. G. Wagner, Y. Jiang, K. Faber, R. J. Kazlauskas, *Angew. Chem.* **2008**, *120*, 8912–8923; *Angew. Chem. Int. Ed.* **2008**, *47*, 8782–8793.

[8] A. Mezzetti, J. Schrag, C. S. Cheong, R. J. Kazlauskas, *Chem. Biol.* **2005**, *12*, 427–437.

[9] Y. Lim, W. Lee, *Tetrahedron Lett.* **1995**, *36*, 8431–8434; W. K. Lee, C. S. Park, Y. H. Lim, H.-J. Ha, Kor. Pat. No. 1005540850000 or, **2002** WO 0212186.

[10] A. J. Repta, M. J. Baltezor, P. C. Bansal, *J. Pharm. Sci.* **1976**, *65*, 238–242; D. D. Miller, F.-L. Hsu, R. R. Ruffolo, Jr., P. N. Patil, *J. Med. Chem.* **1976**, *19*, 1382–1384; Aldrich Catalogue Number 412562 [α]$_D^{20}$ = −4 (*c* 20, H$_2$O).

[11] J. Uppenberg, N. Öhrner, M. Norin, K. Hult, G. J. Kleywegt, S. Patkar, V. Waagen, T. Anthonsen, T. A. Jones, *Biochemistry* **1995**, *34*, 16838–16851.

[12] T. Steiner, W. Saenger, *Acta Crystallogr.* **1991**, *B47*, 1022–1023.

[13] A. Magnusson, K. Hult, M. Holmquist, *J. Am. Chem. Soc.* **2001**, *123*, 4354–4355.

[14] H. J. Yoon, Y.-W. Kim, B. K. Lee, W. K. Lee, Y. Kim, H.-J. Ha, *Chem. Commun.* **2007**, 79–81.

[15] C. S. Park, M. S. Kim, T. B. Sin, D. K. Pyun, C. H. Lee, D. Choi, W.-K. Lee, J.-W. Chang, H.-J. Ha, *J. Org. Chem.* **2003**, *68*, 43–49.

[16] D. Rotticci, F. Haeffner, C. Orrenius, T. Norin, K. Hult, *J. Mol. Catal. B* **1998**, *5*, 267–272; F. Haeffner, T. Norin, K. Hult, *Biophys. J.* **1998**, *74*, 1251–1262; D. Rotticci, J. C. Rotticci-Mulder, S. Denman, T. Norin, K. Hult, *ChemBioChem* **2001**, *2*, 766–770; A. O. Magnusson, M. Takwa, A. Hamberg, K. Hult, *Angew. Chem.* **2005**, *117*, 4658–4661; *Angew. Chem. Int. Ed.* **2005**, *44*, 4582–4585; V. Léonard, L. Fransson, S. Lamare, K. Hult, M. Graber, *ChemBioChem* **2007**, *8*, 662–667.

[17] D. L. Hughes, J. J. Bergan, J. S. Amato, M. Bhupathy, J. L. Leazer, J. M. McNamara, D. R. Sidler, P. J. Reider, E. J. Grabowski, *J. Org. Chem.* **1990**, *55*, 6252–6259; P. E. Sonnet, M. W. Baillargeon, *Lipids* **1991**, *26*, 295–300; T. Lee, J. B. Jones, *J. Am. Chem. Soc.* **1997**, *119*, 10260–10268; H.-J. Ha, K.-N. Yoon, S.-Y. Lee, Y.-S. Park, M.-S. Lim, Y.-G. Yim, *J. Org. Chem.* **1998**, *63*, 8062–8066.

[18] Although these authors did not highlight the different binding mode, their explanation of enantioselectivity used the umbrella-like binding: K. Nishizawa, Y. Ohgami, N. Matsuo, H. Kisida, H. Hirohara, *J. Chem. Soc. Perkin Trans. 2* **1997**, 1293–1298.

[19] A. D. Mesecar, D. E. Koshland, *Nature* **2000**, *403*, 614–615; *Nature* **2000**, *408*, 668; A. D. Mesecar, D. E. Koshland, *IUBMB Life* **2000**, *49*, 457–466; G. Klebe in *Handbook of Experimental Pharmacology, Vol. 153: Stereochemical Aspects of Drug Action and Disposition* (Eds.: M. Eichelbaum, B. Testa, A. Somogyi), Springer, New York, **2003**, pp. 183–198; J. Fokkens, G. Klebe, *Angew. Chem.* **2006**, *118*, 1000–1004; *Angew. Chem. Intl. Ed.* **2006**, *45*, 985–989.

[20] P. Dauber-Osguthorpe, V. A. Roberts, D. J. Osguthorpe, J. Wolff, M. Genest, A. T. Hagler, *Proteins Struct. Funct. Genet.* **1988**, *4*, 31–47.

[21] Examples of X-ray crystal structures showing pyramidal configuration of *N*-alkyl aziridines: K.-D. Lee, J.-M. Suh, J.-H. Park, H.-J. Ha, W. G. Choi, C. S. Park, W. K. Lee, Y. Dong, H. Yun, *Tetrahedron* **2001**, *57*, 8267–8276; Y. Dong, H. Yun, C. S. Park, W. K. Lee, H.-J. Ha, *Acta Crystallogr. Sect. D Biol. Crystallogr.* **2003**, *59*, 659–660; H.-Y. Noh, S.-W. Kim, S. I. Paek, H.-J. Ha, H. Yun, W. K. Lee, *Tetrahedron* **2005**, *61*, 9281–9290.

[22] C.-H. Hu, T. Brinck, K. Hult, *Int. J. Quantum Chem.* **1998**, *69*, 89–103.

[23] C. S. Chen, Y. Fujimoto, G. Girdaukas, C. J. Sih, *J. Am. Chem. Soc.* **1982**, *104*, 7294–7299.